Hindawi
International Journal of Photoenergy
Volume 2020, Article ID 1937040, 9 pages
https://doi.org/10.1155/2020/1937040

Research Article

Experimental Study of a Humidification-Dehumidification Seawater Desalination System Combined with the Chimney

Fei Cao,[1,2] **Qingjun Liu**,[1] **and Hong Xiao**[1]

[1]*College of Mechanical and Electrical Engineering, Hohai University, No. 200, North Jinling Rd., Changzhou 213022, China*
[2]*Sunshore Solar Energy Company Limited, No. 1, Xiting Industrial Park, Nantong 226301, China*

Correspondence should be addressed to Fei Cao; yq.cao@hotmail.com

Received 18 October 2019; Revised 11 February 2020; Accepted 20 February 2020; Published 10 March 2020

Guest Editor: Ting-Zhen Ming

The solar humidification-dehumidification system is of high significance to the freshwater supply in remote areas. In the present study, a humidification-dehumidification seawater desalination system combined with the chimney is designed and experimentally evaluated. Main parameters influencing its freshwater productivity are analyzed. It is found from this study that the cooling tower is required to obtain long-term steady freshwater generation. Raising the temperature difference between the evaporation and condensation chambers would lead to the rise of the freshwater productivity. There is a turning wind speed, beyond which increasing the wind speed would lead to the decline of both the freshwater productivity and the thermal efficiency. The turning wind speed is relevant to the ambient humanity and the heating power. Decreasing the heat power would increase the turning wind speed. When the heating power is 4.9 kW, the highest freshwater productivity and the highest efficiency are 48 g/min and 32.14%, respectively.

1. Introduction

At present, the large-scale applications of seawater desalination mainly include the multieffect distillation, the multistage flash distillation, and the membrane reverse osmosis. These methods are suitable for freshwater demand in large and concentrated areas, as their production cost is closely related to their sizes. However, for some remote areas, i.e., the distributed small islands, the ocean vessels, and the small villages, the freshwater demand is low, dispersion but prerequisite. The small, distributed, low-cost, and less maintenance desalination methods are thus of high significance to solve the problem of freshwater shortage in these areas. However, these areas are always lacking fuel and power. Fortunately, solar energy is available in these areas. Solar energy is then usually used to generate freshwater in these areas. Solar desalination (SD) is a thermal process where solar energy is used to achieve separation of salts from the seawater or brine through evaporation, which is harmless to the environment but requires space for solar energy collection. The SD for freshwater generation is thought to be an effective solution to the water supply at the abovementioned remote areas [1]. The SD process can be generally classified into two categories: the direct system and the indirect system. As a direct system, both the evaporation and the condensation phenomena take place in the same space, which has a simple principle, cheap investment but low efficiency [2]. An indirect system, however, is separated into two chambers, viz., a solar collecting and evaporation chamber and a condensation chamber. This system can achieve the maximum output of freshwater by controlling the operation parameters [3]. The solar humidification-dehumidification seawater desalination system (SHDHSDS) is one kind of indirect SD process. The air is served as the working fluid to transport the evaporated vapor and to generate freshwater.

1.1. Literature Review. Recent studies on the SHDHSDSs mainly focus on the heat transfer enhancement in the evaporators and condensers [4–7], the configuration and operation parameters analyses [8–11], and the experimental studies on demonstration systems [12–19]. Sievers and Lienhard analyzed the heat transfer and fluid flow inside the flat-plate and finned-pipe condensers using numerical simulations [4, 5]. Moumouh et al. fulfilled the heat transfer enhancement

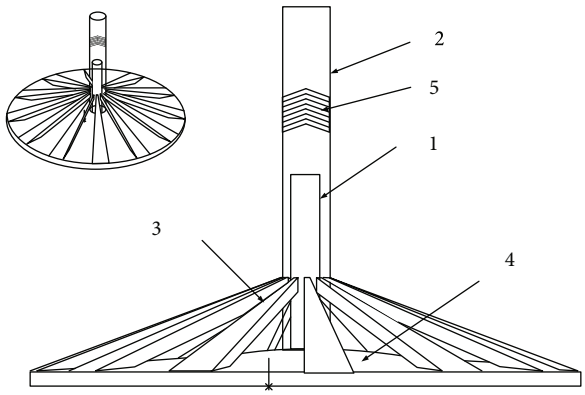

Figure 1: Schematic of the solar double-chimney humidification-dehumidification seawater desalination system (1—inner chimney, 2—outer chimney, 3—sloped solar collector, 4—horizontal solar collector, and 5—condenser).

of flat-plate collectors with siphon water tanks and packed beds through reviewing the SHDHSDSs in the literature [6]. Tariq et al. proposed an innovative air saturator for humidification-dehumidification application that can offer 30% higher freshwater productivity and 11% higher gain output ratio (GOR) as compared to the conventional direct desalination system [7]. Chehayeb et al. analyzed influences of the latent heat recovery on the airflow temperature and the velocity [8]. Sharqawy et al. found that the SHDHSDS with the uniformly supplied total energy needed to be optimized, and they compared two operation strategies of the SHDHSDSs [9]. Yıldırım and Solmus established mathematical models for the SHDHSDS and found that the seawater temperature was one of the main parameters influencing the system performance [10]. Bacha analyzed the transient performance of the SHDHSDS and analyzed the influence of the weather parameters on the system performance [11]. He et al. presented a SHDHSDSs coupled with the heat pump [12]. The simulation results showed that the highest freshwater productivity was 82.12 kg/h. Kabeel et al. constructed a SHDHSDS and analyzed the influences of the inlet and outlet seawater temperatures in the evaporator and the import and export cooling water temperatures on the freshwater productivity. Their experimental results revealed that the freshwater productivity could be up to 23 kg/h when the evaporator inlet temperature reached 90°C [13]. Zamen et al. built a two-stage demonstration SHDHSDS and carried out comparative analysis on their system and the conventional single-stage system. And the freshwater production rate reached 7.25 L/day m^2 [14]. Dayem designed and built a small SHDHSDS with a 1.15 m^2 flat-plate collector and a 400 L water tank. And the freshwater production was 9 L/day [15]. Kabeel and El-Said carried out experimental and simulation studies on a SHDHSDS doping with Al_2O_3 nanoparticles in the seawater. They systematically analyzed influences of the solar radiation, the water flow rate, the inlet water temperature, and the content of nanoparticles on the freshwater productivity. And the maximum freshwater productivity was 41.8 kg/day [16]. Shao et al. carried out experimental study on a small SHDHSDS through exposing the hot air into the solar water heater tank and found that the hot air aeration rate

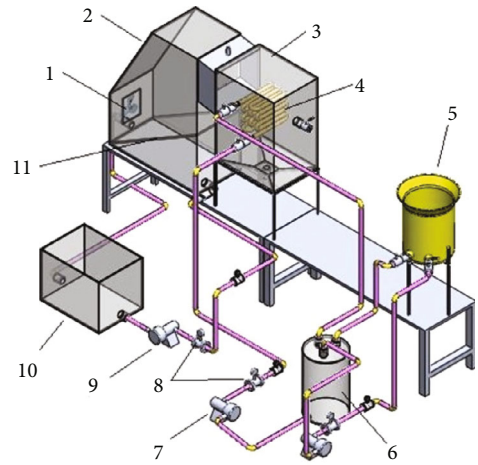

1. Fan
2. Evaporator
3. Condensation chamber
4. Condenser
5. Cooling tower
6. Cooling water tank
7. Cooling water pump
8. Flowmeter
9. Seawater pump
10. Seawater tank
11. Heating plate

Figure 2: 3D figure of the small-scale solar humidification-dehumidification seawater desalination system combined with the chimney.

had positive influence on the temperature and relative humidity at the outlet of the evaporator [17]. Gu combined the solar air collector, the solar water heater, and the condenser together to form a new guide-plate-infiltration SHDHSDS and found that the seawater temperature, the inlet air, and the cooling water flow rates had high influence on the freshwater productivity [18]. Li et al. found the freshwater productivity could be increased by increasing the collector air outlet temperature and relative humidity under the same air velocity and cooling conditions [19].

The experimental demonstration devices validate the feasibility of the SHDHSDS [12–19]. And the literature review indicates that the methods of increasing the freshwater productivity mainly include reasonably increasing the system energy recovery stages [7, 14], increasing the temperatures of the air side and the water side [4–7, 10, 11, 13, 16], increasing the fluid mass flow rate [10, 11, 16], increasing the compactness of the evaporation and condensation devices [4–7], and increasing the heat exchange area [4–7]. However, there is no limit to the total energy input to the systems in the previous study. That is, the air and the liquid temperatures are controlled without considering the consumed energy. And the mutual promotion and the restraint mechanism of the heat transfer and the fluid flow in the humidification-dehumidification processes are seldom considered. For the abovementioned remote areas, the total solar energy is very limited. If more solar energy is used to heat the seawater, the energy used for driving the air and the fluid is less. The problem of reasonable utilization solar energy is of high importance to the SHDHSDS.

1.2. New System Proposal. In order to generate freshwater mainly or only using solar energy, a solar humidification-

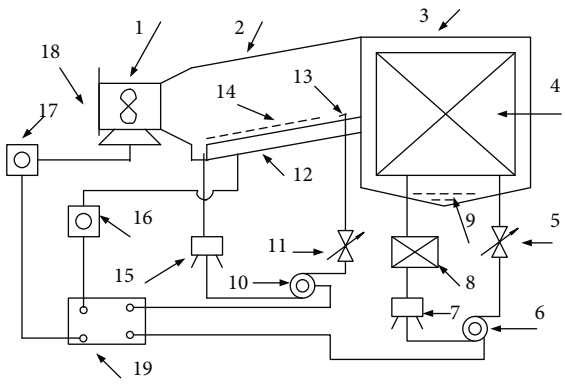

1 -Fan
2 -Evaporation chamber
3 -Condensation chamber
4 -Finned condenser
5 -Valve
6 -Cooling pump
7 -Cooling water tank
8 -Cooling tower
9 -Freshwater
10 -Pump
11 -Valve
12 -Aluminum heating plate
13 -Water segregator
14 -Brine film
15 -Concentrated brine tank
16 -Voltage regulator
17 -Frequency converter
18 -Ambient air inlet
19 -Electrical control cabinet

(a)

(b)

Figure 3: Schematic of the experimental setup: (a) the components and their connections; (b) photo of the experimental setup.

dehumidification seawater desalination system combined with the chimney (SHDHSDSCC) was proposed. Zhou et al. established a one-dimensional compressible flow mode to investigate the power generation and water desalination [20]. Zuo et al. established a small-scale experimental SHDHSDSCC, and the experimental results showed that the SHDHSDSCC can simultaneously achieve the power and the freshwater generation [21, 22]. Ming et al. proposed a mathematical model for the simulation of a SHDHSDSCC with the same size as the Manzanares pilot solar chimney power plant [23]. However, as reported in the literature, the power efficiency of solar chimney is too low, which can hardly be over 1% [24]. And the chimney also has the problems of high construction difficulty [25]. So, it is not cost-beneficial to generate power with the solar chimney in the SHDHSDSCC. As the solar chimney could generate high speed updraft wind, we proposed a new solar double-chimney humidification-dehumidification seawater desalination system as shown in Figure 1. As shown in the figure, the system is composed of five main parts: an inner chimney, an outer chimney, a sloped solar collector, a horizontal collector, and a condenser. The fresh seawater flows along the sloped plate and evaporates inside the sloped solar collector. Ambient air enters into the system from the sloped and the horizontal solar collectors, respectively. The updraft airflow from the horizontal solar collector enters the inner chimney. The wet airflow from the sloped solar collector enters the gas between the inner and outer chimney. The hot air inside the inner and outer chimney mixes with the moist air inside the inner and outer chimney and condenses into freshwater through the condenser, and the remaining air is discharged from the exit of the outer chimney.

Table 1: Parameters of the experimental setup.

Parameter (unit)	Value
Heating plate tilted angle (°)	15
Heating plate area (m^2)	0.78
Ambient air inlet area (m^2)	0.56
Condensation chamber outlet area (m^2)	0.56
Height of evaporation chamber (m)	1.5
Height of the condensation chamber (chimney) (m)	1
Cooling water mass flow rate (kg/h)	1800
Brine mass flow rate (kg/h)	400
Heating power (kW)	3.6/4.9
Ambient temperature (°C)	25
Ambient relative humidity (-)	30%
Power voltage (V)	250/300/330/350
Wind speed (m/s)	0.6/1.3/1.8/2.0/2.2/3.0/3.5

A small-scale SHDHSDSCC is then designed as shown in Figure 2. The seawater is pumped from the seawater tank and sprayed on the surface of the heating plate to form a seawater film on the heating plate. The hot seawater from the heating plate is collected at the bottom of the evaporator and then condensed by the cooling tower and finally stored in the seawater tank. The air drawn from the fan is mixed evenly with the vapor generated from the evaporator to form the moist air. The moist air is heated by the hot water film along the heating plate and flows toward the condenser under buoyancy effect. The moist air is dehumidified in the condenser

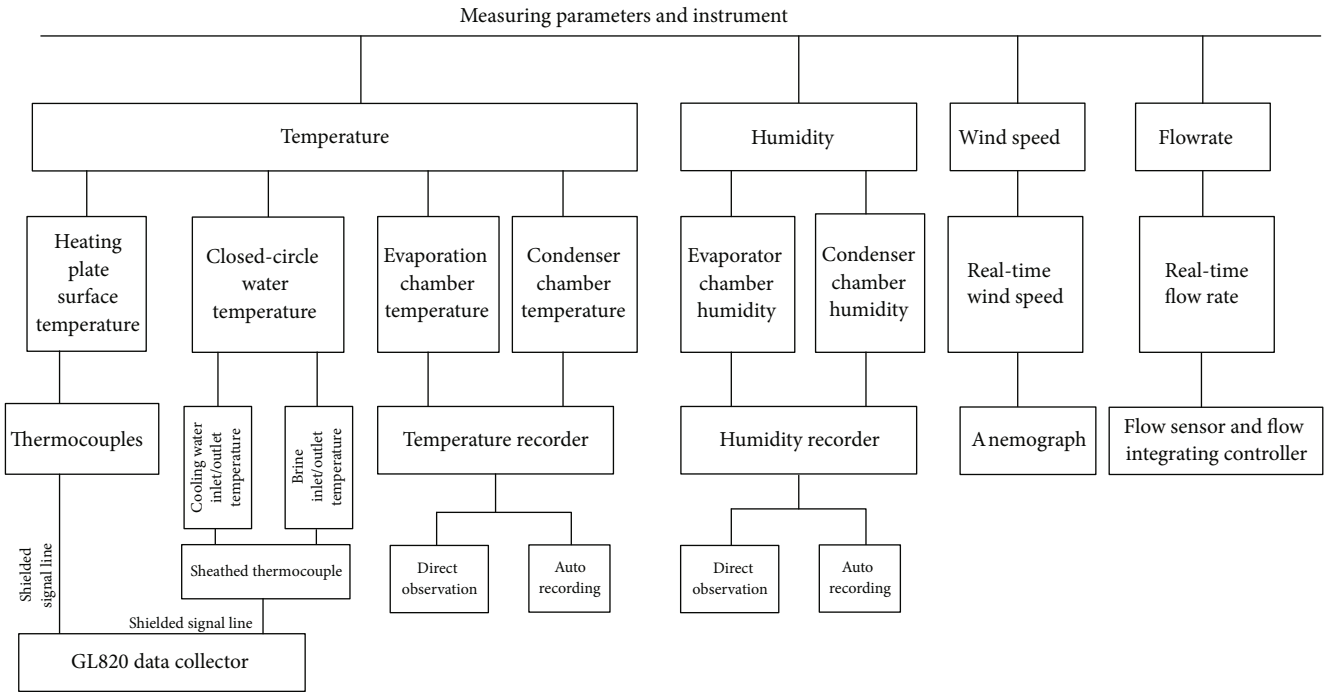

Figure 4: Measuring parameters and instrument in the present study.

Table 2: Parameters of the measuring equipment.

Parameter (unit)	Measure equipment	Range	Accuracy
Temperature (°C)	Type-T thermocouples	(-200, 400)	±0.5
Temperature (°C)	Sheathed thermocouple	(-40, 350)	±0.75%
Humidity (%) and temperature (°C)	TH11R temperature and humidity recorder (with software)	Temperature (-20, 80) Humidity (0,100)	Temperature ±0.5°C Humidity ±3%RH
Wind speed (m/s)	HT-9829 thermosensitive anemometer	(0.1, 25)	±5%
Mass flow rate (m^3/h)	LWGY turbine flow sensor	(0, 6)	±0.5%

by the cooling water to produce freshwater. The rest of the moist air flows out of the condenser and enters the environment. The cooling water is reused and its temperature is controlled by a cooling tower. An experimental setup is then constructed. And the parameters influence the freshwater productivity; i.e., the air and the fluid temperatures, fluid flow rates, and the power consumptions are finally estimated.

2. Experimental Setup

2.1. System Design. An experimental setup is designed according to Figure 2. The schematic and the photo of the experimental setup are shown in Figures 3(a) and 3(b), respectively. In this system, the ambient air enters the evaporation chamber through the ambient air inlet. A fan is set at the ambient air inlet in case of too low wind speed to drive the moist air from the evaporation chamber to the condensation chamber. The air flows through the evaporation chamber, where it accepts the vapor and temperature rises. The high-humidity air then enters the condensation chamber and is condensed by the cooling water. The freshwater is generated at the surface of the cooling water pipelines and is collected by a tank. The rest of the moist air flows out of the condensation chamber towards the environment. The brine is pumped from a tank and is sprayed on a tilted aluminum plate. The tilted plate has inner heating source which can heat the whole aluminum plate. The hot brine water is collected and stored in the tank. The cooling water is circularly used to condense the moist airflow.

A transparent cover is set at the top of the evaporation chamber. The solar radiation can transfer into the evaporation chamber and heats the tilted plate. In order to systematically analyze the parameters influencing the freshwater productivity, the electrical power is used to simulate the solar radiation in the present indoor study. The heating power is controlled by a voltage regulator. And the fan power is controlled by a frequency converter. The mass flow rates of the cooling water and the brine are adjusted using the frequency converter. Detailed parameters of the experimental setup are summarized in Table 1.

2.2. Measurement and Recording. The measuring parameters and instrument in the present study are summarized in Figure 4. As shown in the figure, the air temperatures, relative humanities, brine and water temperatures, and brine firm temperatures are measured by the thermocouples. The

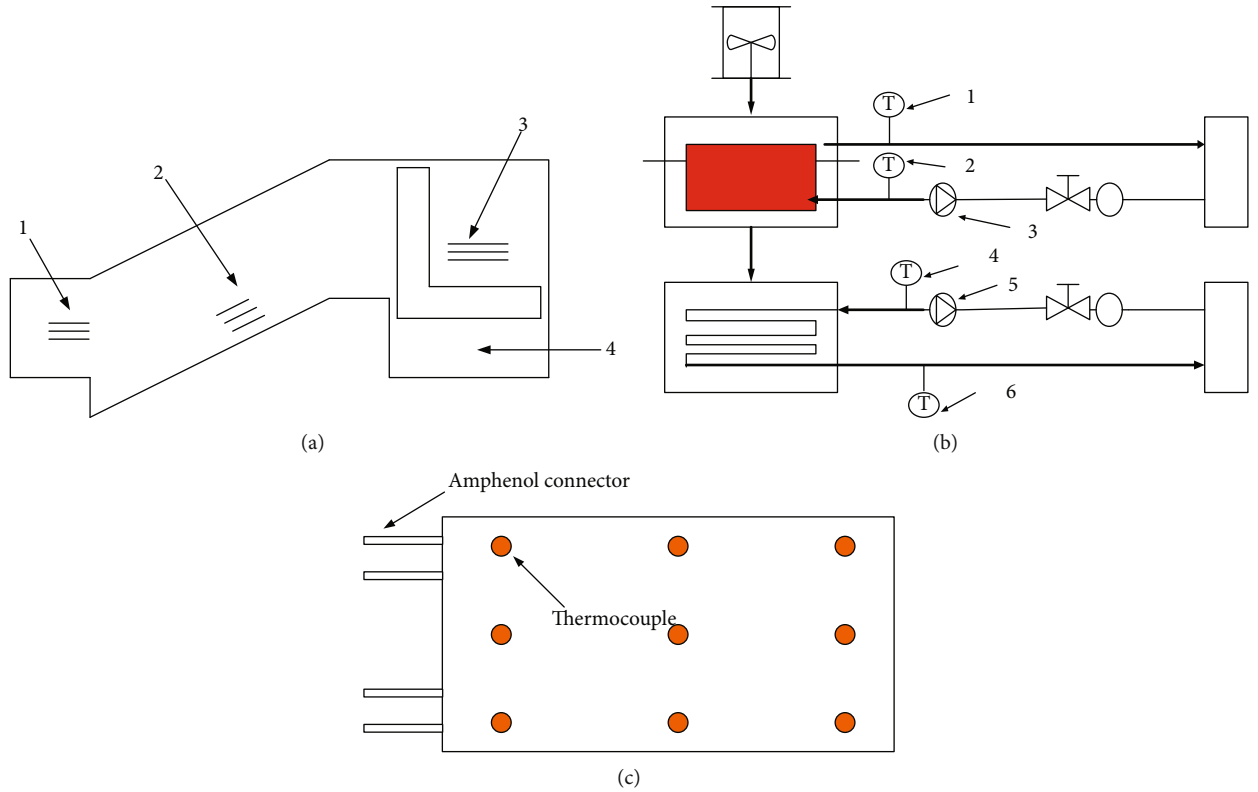

Figure 5: Measuring locations of main parameters in this study: (a) temperature and relative humanity measurement points in 1—the ambient air inlet, 2—the evaporation chamber, 3—the condensation chamber, and 4—the freshwater generate section; (b) measurement location of 1—the brine outlet temperature, 2—the brine inlet temperature, 3—the brine flow rate, 4—the cooling water inlet temperature, 5—the cooling water flow rate, and 6—the cooling water outlet temperature; (c) the thermocouple locations at the surface of the heating plate to measure the brine firm temperature.

cooling water and brine flow rates are measured by the turbine flowmeter. The wind speed is measured by the anemograph. Details of the measurement instrument, i.e., the type, the range, and the accuracy, are supplied in Table 2. The measured signals are recorded by a data recorder. Detailed locations of the measurement parameters are shown in Figure 5.

3. Results and Discussion

3.1. Temperatures. The temperatures in the evaporation and condensation chambers are shown in Figure 6(a). It is found that with the rise of the inlet wind speed, the temperatures inside the evaporation chamber regularly decrease. However, the tendency of temperatures inside the condensation chamber is irregular. The long-term cooling water inlet temperature is shown in Figure 6(b). It can be found that the reason for the irregular tendency of temperatures inside the condensation chamber is that the cooling water temperature increases as it receives heat from the moist airflow inside the condensation chamber. In order to decrease the cooling water temperature, a cooling tower is utilized in this system. With utilization of the cooling tower, the brine and the cooling water temperatures at the inlets and outlets of the evaporation and condensation chambers are shown in Figure 6(c). It is found that the cooling water temperatures are steady during the experiment period. So, though the total energy in the experimental setup is not high, the cooling tower is required to guarantee long-term steady freshwater generation.

3.2. Freshwater Productivity and Efficiency. The freshwater productivities and system thermal efficiencies under different inlet wind speeds are shown in Table 3. It is found that with the increase of the inlet wind speed, the freshwater productivity first increases then decreases, with the peak of 26 g/min at a wind speed of 1.8 m/s. When the wind speed is low, increasing the wind speed could drive more moist airflow into the condensation chamber, leading to the rise of the freshwater generation. However, too high wind speed would drive too much moist air into the condensation chamber in a short time. The moist airflow could not be completely condensed. Much moist air flows out of the condensation chamber, which leads to the decrease of freshwater generation. It is also found from Table 3 that tendency of the thermal efficiency is similar to that of the freshwater productivity. The highest thermal efficiency reaches 21.70%.

3.3. Parameter Analysis

3.3.1. Influence of the Temperature Difference. The freshwater productivities under different temperature differences between the evaporation and condensation chambers are shown in Table 4. It is found that raising the temperature

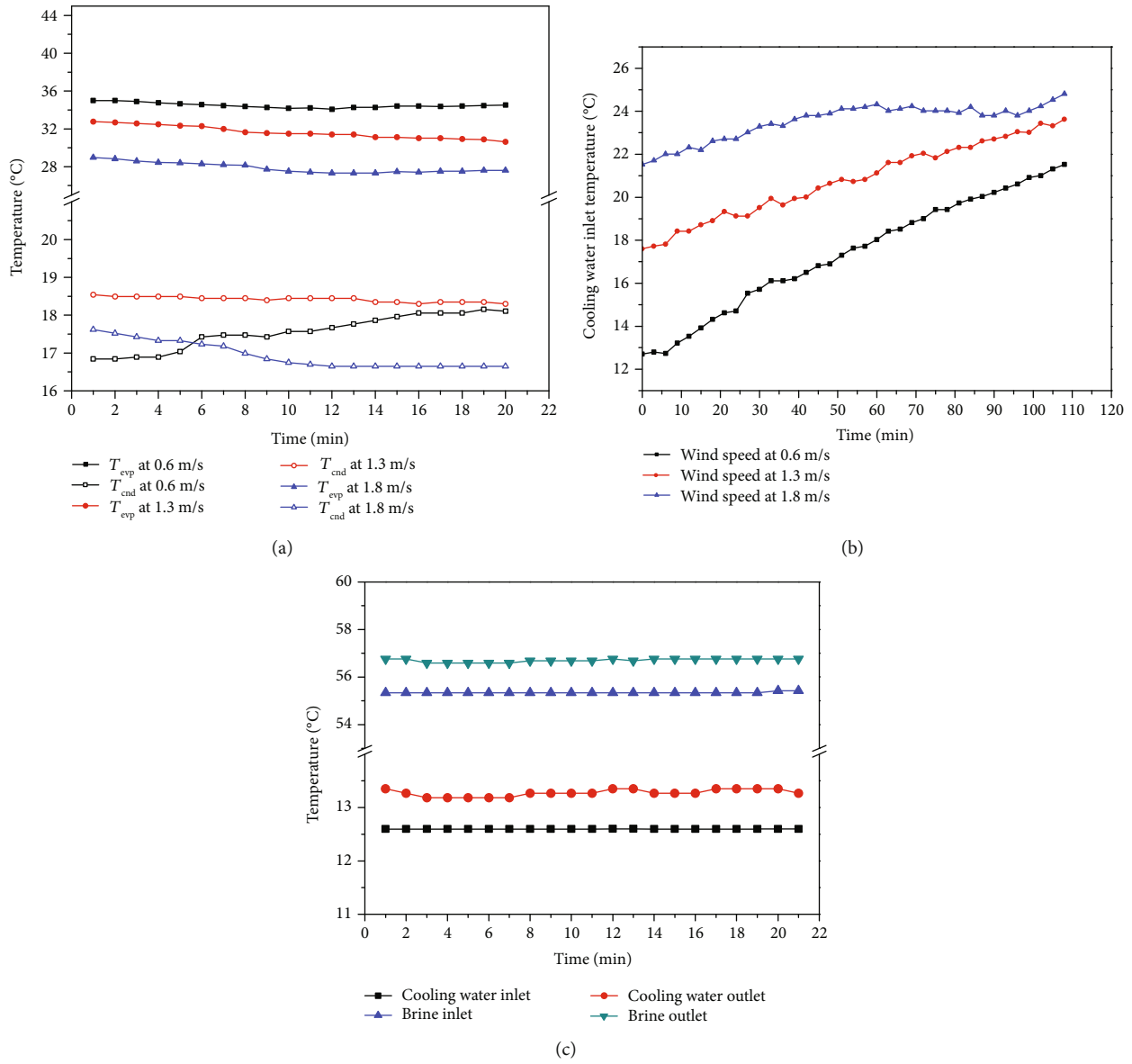

Figure 6: (a) Temperatures in the evaporation and condensation chambers under different wind speeds without a cooling tower (T_{evp} denotes the evaporation chamber temperature, T_{cnd} denotes the condensation chamber temperature, and the speed denotes the wind speed); (b) long-term cooling water inlet temperature without the cooling tower; (c) the brine and the cooling water temperatures at the inlets and outlets of the evaporation and condensation chambers with utilization of the cooling tower.

Table 3: Freshwater productivities and thermal efficiencies under different inlet wind speeds.

Wind speed (m/s)	Freshwater productivity (g/min)	Efficiency (%)
0.6	22	18.60
1.3	24	20.01
1.8	26	21.70
2.0	25	20.80
2.2	24	19.80

Table 4: Freshwater productivities under different temperature differences between the evaporation and condensation chambers.

Temperature difference between the evaporation and condensation chambers (°C)	Freshwater productivity (g/min)
3.44	2.5
3.94	4.7
4.64	5.7
5.15	5.9
6.78	6.6
7.18	6.9
8.69	7.5

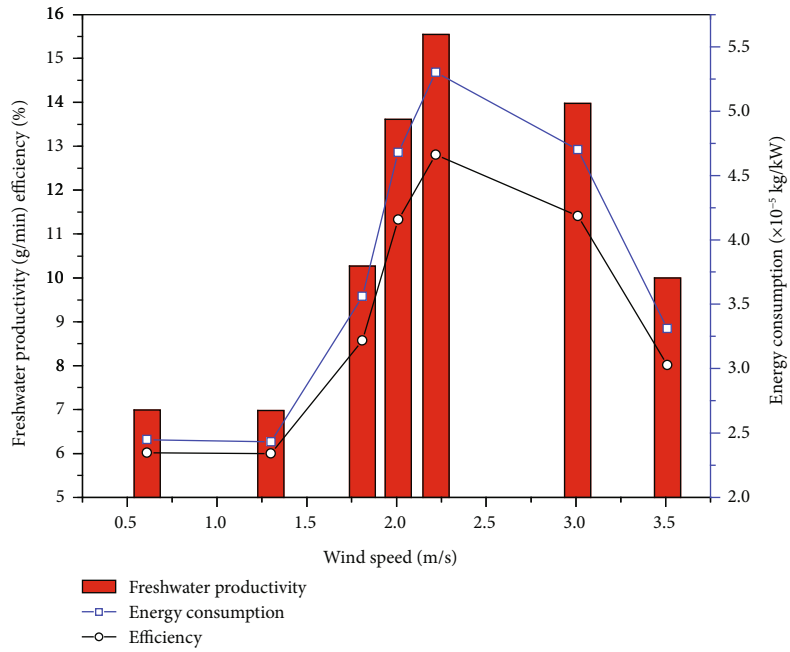

Figure 7: Freshwater productivities, thermal efficiencies, and energy consumption under different inlet wind speeds when the ambient relative humidity is 60%.

difference between the evaporation and condensation chambers would lead to the rise of the freshwater productivity. But it is also observed from Table 4 that the rising rate decreases with the rise of temperature difference between the evaporation and condensation chambers.

3.3.2. Influence of the Ambient Humidity. The freshwater productivities, thermal efficiencies, and energy consumption under different inlet wind speeds when the ambient relative humidity is 60% are shown in Figure 7. Comparing Table 3 (whose ambient relative humidity is 30%) and Figure 7, it is found that the ambient humidity has significant influence on the freshwater productivity. Tendencies of the freshwater productivity under different ambient humidity are similar, both increasing first and then decreasing. When the ambient relative humidity is 60%, the highest freshwater productivity is 16 g/min, which is smaller than that at lower ambient relative humidity. And the highest freshwater productivity occurs when the wind speed is 2.4 m/s. The reason is that the ambient humidity influences both the airflow at the inlet of the evaporation chamber and at the outlet of the condensation chamber. When the ambient humidity is high, less moist air could be condensed in the condensation chamber, which leads to the decrease of the freshwater productivity. It is also found from Figure 7 that tendency of the system thermal efficiency when the ambient relative humidity is 60% is similar with that of the freshwater productivity, whose peak value is 12.7%. And the system thermal efficiency is lower when the ambient relative humidity is higher. Tendency of the freshwater generation under the same energy consumption is similar to that of the freshwater productivity and the thermal efficiency. The highest freshwater generation per kW is 5.30×10^{-5} kg.

3.3.3. Influence of the Heating Power. The freshwater productivities, thermal efficiencies, and energy consumption under different heating power conditions are shown in Figure 8. Two heating powers, viz., 3.6 kW and 4.9 kW, are considered as the low-power condition and the high-power condition, respectively. It is found that increasing the heating power condition has positive influence to the freshwater productivity, as the freshwater productivities under different inlet wind speeds all increase with the rise of heating power. The highest freshwater productivity at high-power condition is 48 g/min. Tendencies of the freshwater productivities and thermal efficiencies under different heating power conditions are similar, both increasing first then decreasing. However, the turning wind speed is not the same, as the highest freshwater productivity at high-power condition locates at the wind speed of 1.3 m/s whereas the highest freshwater productivity at low-power condition locates at the wind speed of 1.8 m/s. In addition, at the high-power condition, higher freshwater productivities are obtained at low wind speeds. And decreasing the heating power would lead to higher freshwater productivity at high wind speeds. The reason is the balance of heat transfer and fluid flow inside the system. When the heating power is high, more brine is evaporated in the evaporation chamber. If the wind speed is too high, much moist air cannot be fully condensed but drawn out of the condensation chamber. When the heating power is low, increasing the wind speed can enhance the heat and mass transfer at the cooling water pipeline surface, which could lead to higher freshwater generation. Tendencies of the freshwater generation under the same energy consumption are similar not only at both high- and low-power conditions but also at different turning wind speeds. The highest freshwater generation per kW at high-power condition is

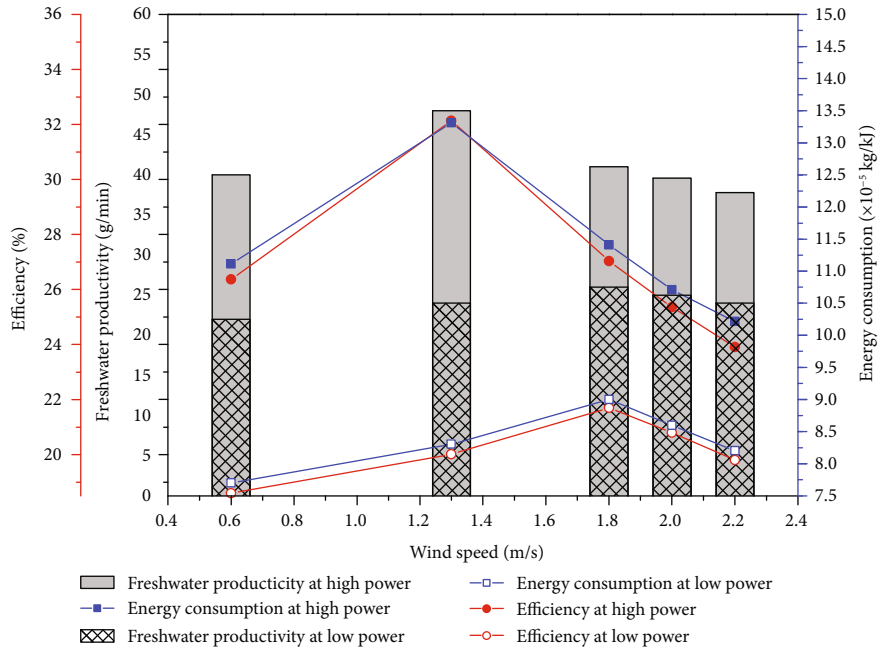

Figure 8: Freshwater productivities, thermal efficiencies, and energy consumption under different heating powers.

13.31×10^{-5} kg. And the highest thermal efficiency under high-power condition is 32.14%.

4. Conclusions

The solar humidification-dehumidification system is of high significance to the freshwater supply in remote areas. In the present study, a solar double-chimney humidification-dehumidification seawater desalination system is proposed. An experimental setup is designed and constructed to obtain the main parameters influencing the freshwater productivity. The following can be concluded from this study:

(1) The cooling tower is required to obtain long-term steady freshwater generation though the obtained energy in the SHDHSDS is low. Raising the temperature difference between the evaporation and condensation chambers would lead to the rise of the freshwater productivity

(2) Tendencies of the freshwater productivities, thermal efficiencies, and energy consumption under different wind speeds are similar. There are turning wind speeds, exceeding in which increasing the wind speed would decrease both the freshwater productivity and the thermal efficiency. And the turning wind speed is relevant to the ambient humanity and the heating power

(3) Decreasing the heat power would increase the turning wind speed. At the high-power condition when the heating power is 4.9 kW, the highest freshwater productivity reaches 48 g/min, the highest freshwater generation per kW is 13.31×10^{-5} kg, and the highest thermal efficiency is 32.14%

Data Availability

The data used to support the findings of this study are included within the article.

Conflicts of Interest

The authors declare that they have no conflicts of interest.

Acknowledgments

This research was funded by the National Natural Science Foundation of China (no. 51506043) and the Fundamental Research Funds for the Central Universities (no. 2019B21914).

References

[1] S. Kalogirou, "Seawater desalination using renewable energy sources," *Progress in Energy and Combustion Science*, vol. 31, no. 3, pp. 242–281, 2005.

[2] M. Chandrashekara and A. Yadav, "Water desalination system using solar heat: a review," *Renewable and Sustainable Energy Reviews*, vol. 67, pp. 1308–1330, 2017.

[3] M. Shatat, M. Worall, and S. Riffat, "Opportunities for solar water desalination worldwide: review," *Sustainable Cities and Society*, vol. 9, pp. 67–80, 2013.

[4] M. Sievers and J. H. Lienhard V, "Design of plate-fin tube dehumidifiers for humidification–dehumidification desalination systems," *Heat Transfer Engineering*, vol. 36, no. 3, pp. 223–243, 2014.

[5] M. Sievers and J. H. Lienhard V, "Design of flat-plate dehumidifiers for humidification-dehumidification desalination systems," *Heat Transfer Engineering*, vol. 34, no. 7, pp. 543–561, 2013.

[6] J. Moumouh, M. Tahiri, and M. Salouhi, "Solar thermal energy combined with humidification-dehumidification process for desalination brackish water: technical review," *International Journal of Hydrogen Energy*, vol. 39, no. 27, pp. 15232–15237, 2014.

[7] K. M. Chehayeb, G. Prakash Narayan, S. M. Zubair, and J. H. Lienhard V, "Use of multiple extractions and injections to thermodynamically balance the humidification dehumidification desalination system," *International Journal of Heat and Mass Transfer*, vol. 68, pp. 422–434, 2014.

[8] R. Tariq, N. A. Sheikh, J. Xamán, and A. Bassam, "An innovative air saturator for humidification-dehumidification desalination application," *Applied Energy*, vol. 228, pp. 789–807, 2018.

[9] M. H. Sharqawy, M. A. Antar, S. M. Zubair, and A. M. Elbashir, "Optimum thermal design of humidification dehumidification desalination systems," *Desalination*, vol. 349, pp. 10–21, 2014.

[10] C. Yıldırım and I. Solmus, "A parametric study on a humidification-dehumidification (HDH) desalination unit powered by solar air and water heaters," *Energy Conversion and Management*, vol. 86, pp. 568–575, 2014.

[11] H. B. Bacha, "Dynamic modeling and experimental validation of a water desalination prototype by solar energy using humidification dehumidification process," *Desalination*, vol. 322, pp. 182–208, 2013.

[12] W. F. He, D. Han, and C. Ji, "Investigation on humidification dehumidification desalination system coupled with heat pump," *Desalination*, vol. 436, pp. 152–160, 2018.

[13] A. E. Kabeel, M. H. Hamed, Z. M. Omara, and S. W. Sharshir, "Experimental study of a humidification-dehumidification solar technique by natural and forced air circulation," *Energy*, vol. 68, pp. 218–228, 2014.

[14] M. Zamen, S. M. Soufari, S. A. Vahdat et al., "Experimental investigation of a two-stage solar humidification- dehumidification desalination process," *Desalination*, vol. 332, no. 1, pp. 1–6, 2014.

[15] A. M. Abdel Dayem, "Efficient solar desalination system using humidification/dehumidification process," *Journal of Solar Energy Engineering*, vol. 136, no. 4, 2014.

[16] A. E. Kabeel and E. M. S. El-Said, "A hybrid solar desalination system of air humidification, dehumidification and water flashing evaporation: part II. Experimental investigation," *Desalination*, vol. 341, pp. 50–60, 2014.

[17] L. T. Shao, X. D. Liu, and Q. L. Liu, "Experimental research on humidification-dehumidification solar seawater desalination device," *Science Technology and Engineering*, vol. 12, pp. 7844–7848, 2012.

[18] F. Gu, *Research on Humidification-Dehumidification Solar Seawater Desalination Technology*, Jiangsu University, Zhenjiang, 2013.

[19] X. Li, G. F. Yuan, Z. Wang, H. Li, and Z. Xu, "Experimental study on a humidification and dehumidification desalination system of solar air heater with evacuated tubes," *Desalination*, vol. 351, pp. 1–8, 2014.

[20] X. Zhou, B. Xiao, W. Liu, X. Guo, J. Yang, and J. Fan, "Comparison of classical solar chimney power system and combined solar chimney system for power generation and seawater desalination," *Desalination*, vol. 250, no. 1, pp. 249–256, 2010.

[21] L. Zuo, Y. Zheng, Z. Li, and Y. Sha, "Solar chimneys integrated with sea water desalination," *Desalination*, vol. 276, no. 1-3, pp. 207–213, 2011.

[22] L. Zuo, Y. Yuan, Z. Li, and Y. Zheng, "Experimental research on solar chimneys integrated with seawater desalination under practical weather condition," *Desalination*, vol. 298, pp. 22–33, 2012.

[23] T. Ming, T. Gong, R. K. de Richter, C. Cai, and S. A. Sherif, "Numerical analysis of seawater desalination based on a solar chimney power plant," *Applied Energy*, vol. 208, pp. 1258–1273, 2017.

[24] F. Cao, L. Zhao, H. Li, and L. Guo, "Performance analysis of conventional and sloped solar chimney power plants in China," *Applied Thermal Engineering*, vol. 50, no. 1, pp. 582–592, 2013.

[25] F. Cao, T. Yang, Q. Liu, T. Zhu, H. Li, and L. Zhao, "Design and simulation of a solar double-chimney power plant," *Renewable Energy*, vol. 113, pp. 764–773, 2017.